The Journal of Experimental Biology 210, 971-982
Published by The Company of Biologists 2007
doi:10.1242/jeb.02728

Limitations to maximum running speed on flat curves

Young-Hui Chang[1,*] and Rodger Kram[2]

[1]*Comparative Neuromechanics Laboratory, School of Applied Physiology, Georgia Institute of Technology, Atlanta, GA 30332-0356, USA and* [2]*Locomotion Laboratory, Department of Integrative Physiology, University of Colorado, Boulder, CO 80309-0354, USA*

*Author for correspondence (e-mail: yh.chang@gatech.edu)

Accepted 17 January 2007

Summary

Why is maximal running speed reduced on curved paths? The leading explanation proposes that an increase in lateral ground reaction force necessitates a decrease in peak vertical ground reaction force, assuming that maximum leg extension force is the limiting factor. Yet, no studies have directly measured these forces or tested this critical assumption. We measured maximum sprint velocities and ground reaction forces for five male humans sprinting along a straight track and compared them to sprints along circular tracks of 1, 2, 3, 4 and 6 m radii. Circular track sprint trials were performed either with or without a tether that applied centripetal force to the center of mass. Sprinters generated significantly smaller peak resultant ground reaction forces during normal curve sprinting compared to straight sprinting. This provides direct evidence against the idea that maximum leg extension force is always achieved and is the limiting factor. Use of the tether increased sprint speed, but not to expected values. During curve sprinting, the inside leg consistently generated smaller peak forces compared to the outside leg. Several competing biomechanical constraints placed on the stance leg during curve sprinting likely make the inside leg particularly ineffective at generating the ground reaction forces necessary to attain maximum velocities comparable to straight path sprinting. The ability of quadrupeds to redistribute function across multiple stance legs and decouple these multiple constraints may provide a distinct advantage for turning performance.

Key words: turning, maneuverability, curve, sprinting, running, locomotion, biomechanics.

Introduction

In nature, evasive maneuvers associated with high-speed predator/prey chases are often a priority in locomotor performance. For example, predators with faster straight-ahead running speeds cannot catch their prey if they are unable to maintain a sufficient fraction of their speed along a curved path during a pursuit. If the slower prey waits until the last possible instant before performing a turning maneuver, it can avoid being caught. There have been a few studies of curved path sprinting and maneuverability during controlled conditions (Walter, 2003; Usherwood and Wilson, 2005) and natural predator avoidance (Alexander, 1982; Howland, 1974), but more detailed biomechanical data such as ground contact forces generated by the limbs are lacking. Such data are difficult to obtain in non-human animals. Studying curve sprinting in humans provides a more tractable experimental system for gaining insights into the fundamental principles that limit sprint speed along curved paths.

The maximum human running speed along a flat curved path is significantly slower relative to a straight path. Records from track and field meets were examined (Jain, 1980) and it was found that 200 m sprinters were up to 0.4 s slower on curved tracks compared to straight tracks. This decrease in maximum speed is related to the curvature of the track lane and can potentially result in one sprinter gaining an advantage of up to 0.12 s over a competitor in an adjacent inside lane (Harrison and Ryan, 2000; Jain, 1980). The attenuation of sprint speed is more pronounced as the radius of curvature is reduced. The mechanism for this speed reduction, however, is not firmly established.

Several studies have attempted to explain this phenomenon by modeling the sprinter as a point mass and using classical physics principles for objects moving in a circular path (Keller, 1973; Mureika, 1997). Along a curved path, the sprinter must generate centripetal forces by applying lateral force on the ground with each step (Fig. 1). This centripetal force is required to change the direction of the momentum vector of the sprinter. Few studies, however, have attempted to combine the physics with the biomechanical limitations of the body to explain the mechanism for sprint speed attenuation during flat curve sprinting.

An innovative model for flat curve sprinting performance was proposed (Greene, 1985) based on the primary assumption of a physiological limit to the maximum leg extension force.

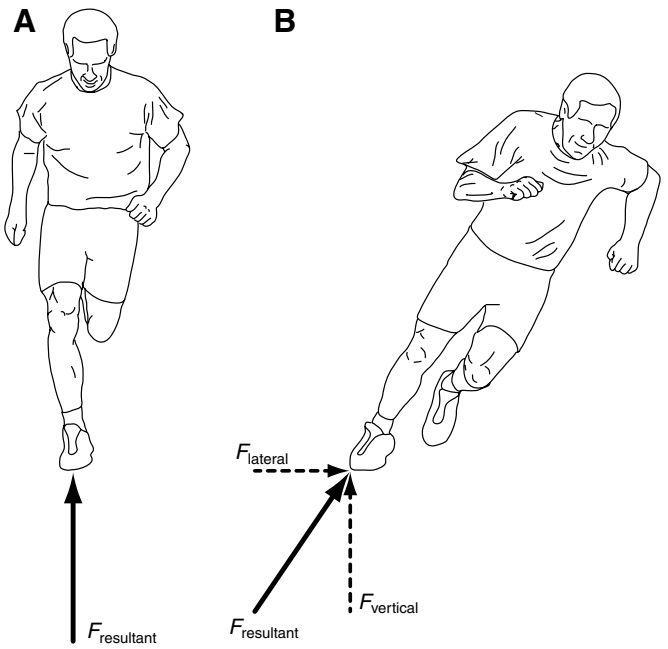

Fig. 1. Ground reaction forces (GRF) in the frontal plane of a sprinter along a straight path (A) and on a curved path (B). Along a straight path, lateral forces ($F_{lateral}$) are negligible and the peak vertical component of the GRF ($F_{vertical}$) equals the peak resultant GRF ($F_{resultant}$). When running along a curved path, $F_{lateral}$ comprises a significant portion of the total resultant force. If the upper limit to $F_{resultant}$ is achieved on the curve as Greene's theory suggested (Greene, 1985), then for the same $F_{resultant}$, $F_{vertical}$ on the curve must be smaller relative to that generated on a straight path. Note that the axis of the fore–aft component of the GRF is coming out of the page in both cases and the fore–aft component is negligible when $F_{resultant}$ is at its peak.

According to Greene, a theoretical limit to peak resultant force exerted on the ground must result in a vectorial decrease in the peak vertical component due to the concomitant increase in the lateral component (Fig. 1). A smaller peak vertical force would require an increase in ground contact time to generate sufficient vertical impulse to support body weight over the entire stride. Running velocity can be calculated as the distance traveled during foot contact (L_C) divided by the contact time of the foot (t_C). Given that L_C does not change substantially with speed (McMahon and Greene, 1979; Weyand et al., 2000), an increase in t_C would reduce forward sprinting velocity. With these basic assumptions, Greene derived a relationship between forward sprint velocity and radius of curvature for small and large radii.

Although his empirical data on maximum running speeds agree with the theory, Greene stated "*there was a significant degree of scatter to [the] data...[making it] possible that other theoretical models [could] predict the data as successfully*" (Greene, 1985). A similar model was developed using the same assumption of a constant leg force to predict human sprint speeds from kinematics data (Usherwood and Wilson, 2006). Yet, in the 20 years since Greene's study, no ground reaction force (GRF) data have been published to test this primary assumption that maximum leg extension forces (i.e. peak resultant ground reaction forces) limit sprint speed on flat curves.

Greene's data were collected on tracks of relatively large radii (11 m and 19 m) (Greene, 1985; Greene, 1987). Although these are realistic dimensions for indoor track events, they are not realistic for predator/prey contexts where much tighter turns are common (Howland, 1974). We reasoned that the general principles of how curvature affects maximum speed running would be more clearly observed at extremely small radii. It is often at these limits of performance that we can gain the greatest insight into the design and function of the locomotor apparatus (Full and Koditschek, 1999).

The primary goal of this project was to directly test the hypothesis that the maximum physiological leg extension force observed during straight path sprinting is also generated during flat curve sprinting. We define 'maximum physiological leg extension force' as being the maximum extension force that an individual is capable of generating and is estimated by the peak resultant ground reaction force measured during straight path sprinting. 'Peak resultant ground reaction force' is defined as the peak force generated by the legs on the ground during a given sprint trial on either a straight or curved path. If the ability of a sprinter to exert a leg extension force on the ground is the limiting factor in maximum velocity, then the peak resultant ground reaction force should remain constant at all curvatures. To gain further insight into what limits maximum speed during curve sprinting, we separated the effects of generating the lateral GRF component from the effects of the curved path itself. According to Greene's theory, if a person were able to sprint along a curved path without having to generate centripetal forces, the sprint speed should not be slower than on a straight path. Specifically, we measured: (i) the constancy of peak resultant GRF for sprinters along curved paths of various radii; and (ii) sprint velocity on curved paths when centripetal forces were supplied by a tether rope secured at the center of a circular track.

A secondary goal of this study was to test the hypothesis that both legs act symmetrically during sprinting on flat turns. The symmetrical action of the legs is an implicit assumption in Greene's theory and other curve sprinting theories that treat the runner as a point-mass (Keller, 1973; Mureika, 1997). Given the differences in muscle activity, limb and joint dynamics observed between legs during discrete 'cutting' maneuvers (Besier et al., 2003; Besier et al., 2001a; Besier et al., 2001b; Ohtsuki and Yanase, 1989; Ohtsuki et al., 1987; Ohtsuki et al., 1988; Rand and Ohtsuki, 2000), we predicted that the biomechanical constraints placed on the inside leg would be different from those placed on the outside leg. We specifically tested for asymmetries in the forces generated on the ground and in the stride kinematics. Asymmetrical biomechanics might suggest that one leg preferentially limits sprint speed on flat curves.

Materials and methods

We collected data on five recreationally fit men between the ages of 25 and 38 years old (29.4±5.2 years, mean ± s.d.). Body mass of subjects ranged from 70.6 to 94.6 kg (80.7±9.0 kg) and leg length ranged from 0.90 to 0.96 m (0.94±0.03 m). All data were collected at the Richmond Field Station of the University of California. Subjects gave their informed consent before participating in this study as per the University of California Committee for the Protection of Human Subjects.

Subjects sprinted on circular tracks of 1, 2, 3, 4 and 6 m radii. All five tracks were drawn with paint on flat, clean, paved asphalt so that they were cotangential with a strategically placed force platform (Advanced Mechanical Technology, Watertown, MA, USA; Fig. 2). The force platform was mounted flush with the surface of the ground and was covered with a rubber matting to prevent slipping. The track was kept clean of debris and subjects wore rubber-soled running shoes to allow maximal effort with no slipping. Subjects also wore safety wrist guards and knee pads for protection and to reduce fear of injury due to slips. We collected ground reaction forces as subjects sprinted on all five curved tracks and also on a straight 30 m runway leading up to the force platform. A 200 Hz high-speed video camera (J.C. Labs, Inc., Mountain View, CA, USA) provided a lateral view of the sprinters as they crossed the force platform. Video records were used to calculate the sprint speeds (Fig. 2).

To apply an external centripetal force to the subjects, we attached a rope near the center of mass *via* a padded hip belt. The rope was attached in front and behind the sprinter to the ends of a light but strong wooden dowel (3 cm diameter, 1 m long) secured to the outside of the hip belt. This triangular frame allowed for free movement of the arms during sprinting, the ability to lean forward and also rotation about the vertical axis. The other end of the rope was tethered to a bearing assembly (model SCHB-24, Bearing Engineering, Emeryville, CA, USA) affixed to a steel pole, which sat in a 30 cm deep steel pipe sleeve mounted in concrete at the center of each track. The height of the bearing assembly was adjusted to match the hip height for each subject. A uniaxial force transducer was placed in series with the tether rope to measure the external force being applied to the subject (model LCCB-1K, Omega Engineering, Santa Ana, CA, USA).

Protocol

After a 30 min warm up and practice session, subjects began by sprinting on the straight path. We measured sprint speed for the last 5 m of the sprint. Subjects then sprinted along the circular tracks alternating between the normal curve sprinting condition and the tethered condition at each radius. Subjects ran between 3–5 trials at each condition. Three subjects started with the largest radius and ended with the smallest radius. Two subjects performed the order in reverse and due to time constraints completed their trials over multiple days. Subjects were given sufficient time to rest between trials. We again measured straight path sprint speeds for each subject at the end of each session to verify that fatigue had not affected their sprint speeds over the course of the trials. No significant differences were found between beginning and end sprint speed measurements (paired *t*-test, $P>0.05$).

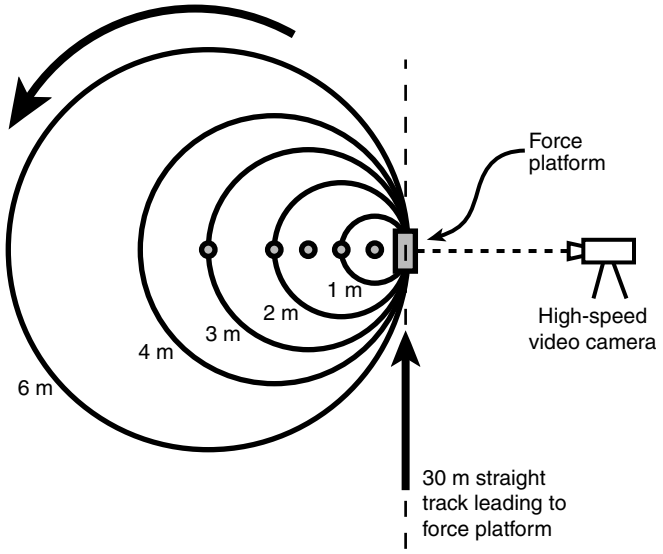

Fig. 2. Overhead view of experimental set-up. Circular lines of 1, 2, 3, 4 and 6 m radius were painted on the ground such that they were all cotangential with a force platform mounted flush with the ground (counter-clockwise sprinting direction, as indicated). We used a 30 m straight runway leading up to the force platform for control trials. A high-speed video camera recorded lateral views of the subjects as they stepped onto the force platform. Pipe sleeves (gray circles) were inserted into the ground to mount a removable steel pole at the center of each track for tethered trials.

Velocity calculations

For straight sprinting trials, velocities were measured by two observers with stopwatches and also by a set of infrared sensors in the last 5 m of the runway before subjects reached the force platform. The averaged stopwatch values compared well with the sensor data. For curved sprinting trials, the sensors were used along secants of the track. Due to sunlight interference, however, we found the infrared sensor measurements to be less reliable on the curved tracks and we discarded them in favor of velocities calculated from video. For the 1 m and 2 m radii, velocity was calculated over one complete revolution (6.3 m and 12.6 m circumference, respectively) starting and ending when the subject's hip marker crossed the center of the force platform, which could be easily identified by the tether pole placed at the center of each circular track. For the 3, 4 and 6 m radii, velocity was calculated over half of a revolution (9.4, 12.6, 18.9 m half circumference, respectively), starting when the subject's hip marker crossed on the exact opposite side of the track from the middle of the force platform as indicated by the tether pole. Each subject's fastest velocity trial was used for maximum sprint speeds at each condition and radius.

Force calculations

We sampled ground reaction force data from the force platform at 1 kHz per channel for the z, y and x components. Vertical, fore–aft and lateral components were then calculated by transforming the global force platform coordinate system (z, y, x) to a local, anatomical coordinate system with its origin based at the center of pressure underneath the foot. The fore–aft direction was defined as tangential to the curved path and the medial–lateral direction was defined as radial to the curved path. In this way, all fore–aft and lateral components of force are relative to the curved path and did not depend on where the foot landed on the force platform. We collected force data for 2–4 steps per sprint trial depending upon the circumference of the track (fewer laps for larger radii resulted in fewer steps). In no trials was the last step the fastest; indicating that we had likely captured the subject's maximum velocity for that condition. We filtered the data with a 4th-order recursive, zero phase-shift, Butterworth low-pass filter with a 25 Hz cut-off. We have previously determined that 99% of the integrated power content of the vertical GRF signal during running is at frequencies <10 Hz and 98% of the horizontal GRF signal is at frequencies <17 Hz (Kram et al., 1998). We also collected and averaged the tether force data.

For each trial, we calculated the peak resultant GRF magnitude, the peak GRF components, and the average force applied on the sprinter by the tether. For each condition, peak resultant forces were averaged across subjects for the outside and inside legs. We determined step length (L_{STEP}, distance from heel-strike to contralateral heel-strike), step frequency (f_{STEP}, inverse of time from heel-strike to contra-lateral heel-strike), and time of ground contact (t_C) from the ground reaction force data. The instant of heel-strike was determined from the vertical force record by finding the closest local minimum before the vertical GRF reached a threshold of 100 N. The instant of toe-off was determined by finding the nearest local minimum after the vertical ground reaction force dropped below 100 N.

Statistical analyses

Due to our limited sample size for each condition, performing a multifactor analysis of variance (ANOVA) would result in the presence of singularities. Instead, we performed a single-factor ANOVA on our sprint speed, peak resultant ground reaction force and stride parameter data. This provided a much more conservative test for differences across all trial conditions since each was treated as an independent observation. When we detected a significant effect, we performed a Tukey's honestly significant difference *post-hoc* test (P=0.05) to further test each radius condition to the straight path, normal curve sprinting to tethered curve sprinting and inside leg to outside conditions. Although this approach put us at risk for a type II error (false negatives), any significant differences found should be quite robust. As an additional test, we pooled our speed and ground reaction force data across all radius conditions and performed a linear regression on the log-transformed data plotted against a log-transformed dimensionless radius (inverse Froude number). We then calculated the 95% confidence intervals (C.I.) of these regression slopes to test for significant trends in the force data across legs or to test if the sprint velocities predicted by Greene's theory fell within the 95% C.I. of our log-transformed velocity data.

Results

Maximum velocity

Maximum sprinting velocity on the curve was significantly slower at all radii compared with the straight path. We observed a significant effect of our experimental curve and tether conditions on maximum sprint velocity ($F_{(10,44)}$=158.51, P<0.001). In a follow-up *post-hoc* test, we found that maximum sprint velocity was slower in all curved path conditions compared to the straight path condition (P<0.05, Fig. 3, Table 1). Also, at each radius condition, the use of the tether resulted in a significantly faster sprint speed compared to normal curve sprinting (P<0.05, Fig. 3, Table 1). For example, compared to the straight path condition, sprint velocity at the 3 m radius was 41.7% slower for normal curve sprinting, but only 32.5% slower with the tether.

Ground reaction forces

Typical ground reaction force data sets from one representative subject are shown for each tether, track radius and leg condition (Fig. 4). Ensemble averages for peak ground reaction force components across all subjects are shown in Fig. 5.

Compared to the straight path, peak vertical ground reaction forces were smaller at the smaller radii for both normal and tethered curve sprinting (Figs 4i, 5i). The inside leg consistently produced smaller peak vertical ground reaction forces than the outside leg at each radius during normal curve sprinting. During tethered trials, however, both legs produced similar peak vertical ground reaction forces.

Peak propulsive ground reaction forces (Figs 4ii, 5ii) decreased at smaller radii during all sprint conditions on the curve compared to the straight path. In normal flat curve sprinting, the outside legs consistently generated greater propulsive forces than the inside legs. In contrast, with a tether, there was no consistent difference between legs with regard to generation of peak propulsive ground reaction forces.

Absolute magnitudes for peak braking ground reaction forces for normal curve sprinting also decreased at smaller radii, with the outside legs generating greater braking forces than the inside legs at each radius. In the tethered condition, however, the outside leg did not show a strong trend with radius, in contrast to the inside leg, which decreased in magnitude with smaller radii.

Peak lateral ground reaction forces (Figs 4iii, 5iii) were significantly greater for normal curve sprinting compared to straight path sprinting, but for all the curve conditions, values did not change substantially with radius. The outside leg always

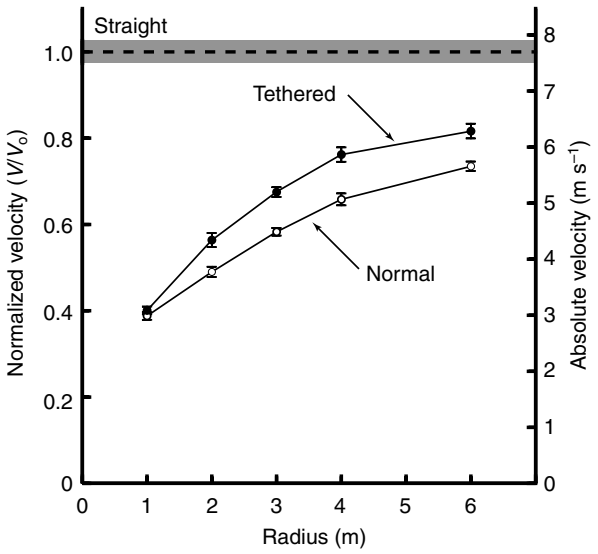

Fig. 3. Maximum sprint velocity as a function of radius for normal curve running (open circles) and tethered running (filled circles). Velocity decreased with decreasing radius. The tether reduced the need to generate centripetal force and increased velocity on the curve, but to magnitudes less than those predicted by Greene (Greene, 1985). Data represent means for five subjects at each condition. Error bars are the s.e.m. for absolute velocities. The broken line indicates mean maximum velocity on straight path (V_o) and the gray band indicates ± s.e.m.

Table 1. *Maximum velocity and corresponding ground reaction forces for each condition*

Track	Maximum velocity (m s^{-1})	Peak resultant force (BW)	
		Inside leg	Outside leg
Straight	7.70±0.20 (5)	2.72±0.16 (5)	2.72±0.16 (5)
Curved radius (m)			
Normal			
6	5.66±0.08*,† (5)	2.48±0.06 (4)	2.63±0.11 (4)
4	5.07±0.11*,† (5)	2.28±0.08 (5)	2.59±0.10 (5)
3	4.49±0.07*,† (5)	2.29±0.12 (5)	2.53±0.10 (5)
2	3.77±0.09*,† (5)	2.07±0.07* (5)	2.43±0.11 (4)
1	2.99±0.07*,† (5)	1.87±0.03* (5)	2.25±0.12 (4)
Tethered			
6	6.29±0.13* (5)	2.79±0.17 (4)	2.77±0.13 (5)
4	5.87±0.13* (5)	2.70±0.14 (4)	2.72±0.15 (5)
3	5.20±0.09* (5)	2.63±0.16 (4)	2.62±0.16 (5)
2	4.34±0.13* (5)	2.33±0.12 (5)	2.44±0.12 (5)
1	3.09±0.07* (5)	2.07±0.10 (3)	2.12±0.10* (5)

BW, body weights.
Values are means ± s.e.m. (number of subjects in parentheses).
*Statistically significant difference to the straight path condition (P<0.05).
†Statistically significant difference to the matched radius, tethered condition (P<0.05).

generated greater peak lateral ground reaction forces at each radius compared to the inside leg. In contrast, with tethered sprinting, we observed a decreasing trend in lateral force at smaller radii but no substantial difference in peak lateral ground reaction forces between the two legs.

Leg extension force

We observed a significant effect of our experimental curve and tether conditions on the peak resultant ground reaction forces generated ($F_{(20,75)}$=4.83, P<0.001). Upon further *post-hoc* analysis, we saw that the outside leg did not generate statistically different forces from those generated during straight path sprinting at any radius for the normal untethered condition (P>0.05). In contrast, the inside leg generated significantly lower peak resultant ground reaction forces at the 1 m and 2 m radius conditions (P<0.05, Fig. 6A, Table 1). For tethered curve sprinting, only the outside leg at the 1 m radius condition showed significantly lower peak resultant ground reaction forces compared to the straight path sprinting. Although a *post-hoc* test (Tukey HSD, α=0.05) did not reveal any significant differences between inside and outside legs at matched radii, we likely lacked the statistical power in the ground reaction force data to resolve any true differences between legs due to the limited number of samples collected at each tether and leg condition. This is supported by the consistent trends in the ground reaction force *vs* radius data (Fig. 6) and the fact that we saw more significant differences in the forces generated by the inside leg compared to the straight path condition.

To further investigate the effect of asymmetrical function of the legs on forces generated against the ground, we pooled all of our peak resultant ground reaction force data across radius conditions and binned them into four groups: one for each leg and tether condition combination. We performed a linear regression on the log transformed peak resultant ground reaction force (GRF) data as a function of log-transformed dimensionless radius (Eqn 1–4), where M_b is body mass, $\boldsymbol{g}$ is the gravitational constant, R is track radius, and V_o is straight path sprint velocity. We then compared the slopes (mean ± half of 95% C.I.) of these regressions for each leg during both normal and tethered curve sprinting.

Normal curve sprinting:

Inside leg:

$$-\log(GRF_{inside}/M_b\boldsymbol{g}) = 0.154(\pm0.0238) \times [-\log(R\boldsymbol{g}/V_o^2)] - 0.392 ; \quad (1)$$

Outside leg:

$$-\log(GRF_{outside}/M_b\boldsymbol{g}) = 0.0889(\pm0.0303) \times [-\log(R\boldsymbol{g}/V_o^2)] - 0.425 . \quad (2)$$

Tethered curve sprinting:

Inside leg:

$$-\log(GRF_{inside}/M_b\boldsymbol{g}) = 0.192(\pm0.0350) \times [-\log(R\boldsymbol{g}/V_o^2)] - 0.459 ; \quad (3)$$

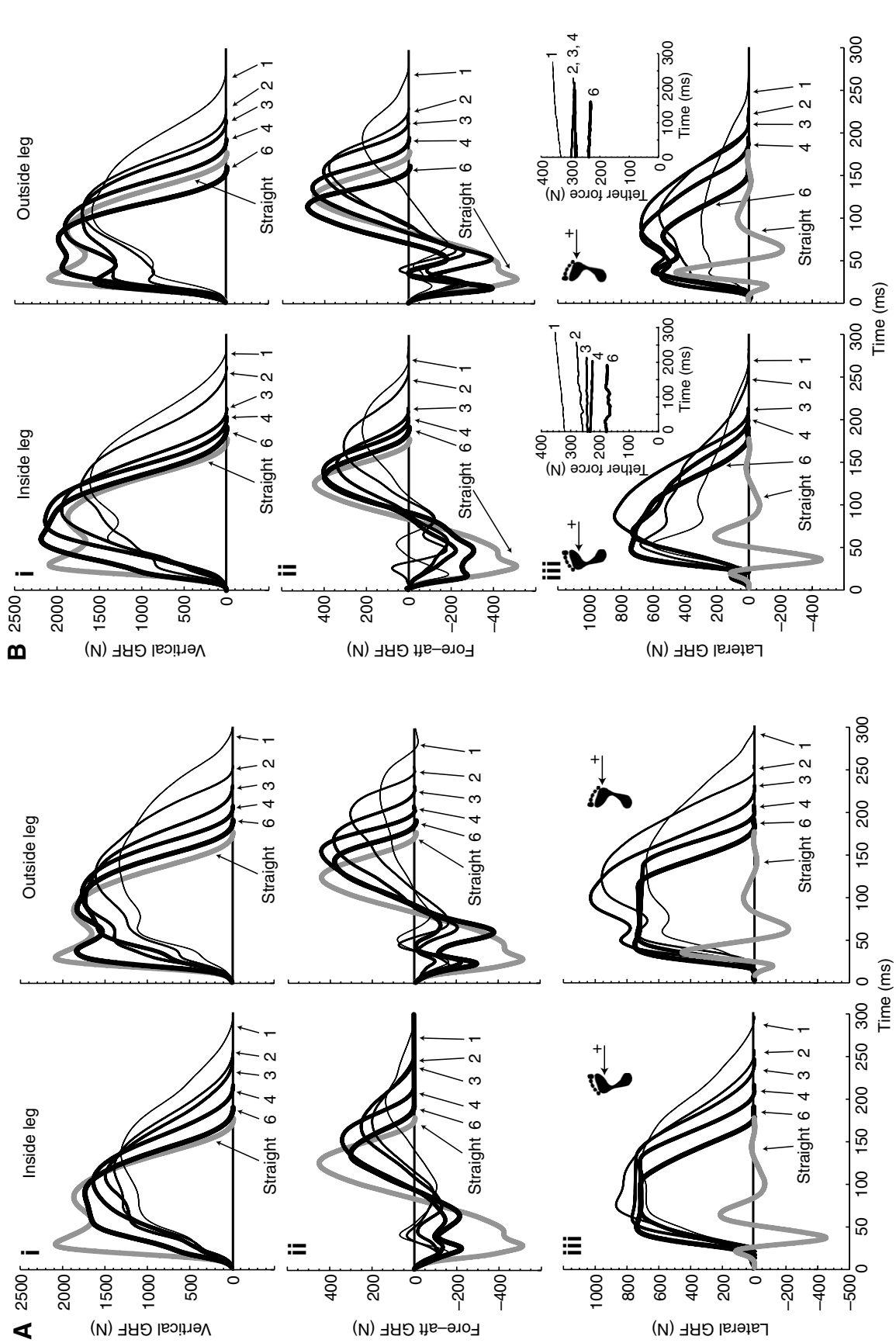

Fig. 4. Representative ground reaction force (GRF) components from typical trials for one subject sprinting at each radius of curvature normally (A) and with a tether supplying external centripetal forces (B). Straight path sprinting is shown for comparison (thick gray lines, symmetry assumed for straight path) and correspondingly smaller radii are indicated by progressively thinner black lines (6, 4, 3, 2, 1 m). The inside leg (left) and outside leg (right) are indicated for each GRF component. (Ai,Bi) Vertical GRF. Fore–aft GRFs (Aii,Bii) indicate negative, braking forces followed by positive, propulsive forces in each case. Positive lateral GRFs (Aiii,Biii) indicate centripetal forces acting at the feet. Corresponding tether forces are shown with indicated curve radius (Biii, inset).

Outside leg:

$$-\log(GRF_{outside}/M_b g) = 0.168(\pm 0.0310) \times [-\log(Rg/V_o^2)] - 0.458 . \quad (4)$$

During normal curve sprinting without the tether (Eqn 1, 2) the peak forces generated by the inside leg decreased twice as much for a given decrease in radius (95% C.I.=0.130–0.178, r^2=0.655) compared to the outside leg (95% C.I.=0.059–0.119, r^2=0.302). In contrast, when sprinting with the tether (Eqn 3, 4) the decrease in force generation by the inside leg (95% C.I.=0.157–0.227, r^2=0.627) and outside leg (95% C.I.=0.137–0.199, r^2=0.559) for a given decrease in radius was the same. The intercept for the inside leg during normal curve sprinting was also lower than that for the outside leg, but comparable during tethered sprinting.

Greene's predictions

Although our velocity data qualitatively support Greene's predictions for the relationship between maximum sprint speed and radius (Fig. 3), they predict a significantly greater exponent for the power fit of the data. Greene predicted a relationship with an exponent of 0.258 for large radii [from equation 12 in Greene (Greene, 1985)] and an exponent of 0.333 for small radii [from equation 42 in Greene (Greene, 1985)]. Our data indicate a power relationship with an exponent of 0.363±0.012 (0.012 represents the 95% C.I. of our data; Eqn 5 and Fig. 7):

$$V_{curve}/V_o = 0.746(Rg/V_o^2)^{0.363\pm0.012} , \quad (5)$$

where V_{curve}/V_o is a dimensionless velocity, in which V_{curve} is the maximum velocity for a given radius and V_o is the maximum velocity on the straight path. Rg/V_o^2 is a dimensionless radius that Greene derived to compare sprinters with different maximum sprint speeds and is equivalent to an inverse Froude number (Greene, 1985).

Kinematics

We saw a significant effect of radius and tether on step length ($F_{(10,38)}$=35.38, P<0.001) and time of ground contact ($F_{(10,38)}$=16.18, P<0.001), but no effect on step frequency ($F_{(10,38)}$=1.83, P>0.05). On a follow-up *post-hoc* analysis, we did not see significant differences in step length or time of ground contact between the inside and outside legs at any condition, but we did find significant differences at each condition compared to the straight path condition (Table 2).

Discussion

Maximum leg force

Here we show that sprint speed on small radius curves is not only limited by a physiological upper limit to leg force. Greene's model characterizing the speed–radius relationship for curve sprinting assumes that "*maximum running effort is mechanically realized as maximum force*" [equation 7 in Greene (Greene, 1985)]. This assumed that the physiological limit to leg force would be generated on the ground at every radius during sprinting. Our empirical evidence disputes that assumption.

Our direct measurements during curve sprinting indicated that the peak resultant ground reaction forces generated during maximal effort straight path sprinting were never reached for the inside leg at the smaller radii tested (Fig. 6, Table 1). Peak resultant ground reaction force decreased more with decreasing radius for the inside leg compared to the outside leg. When sprinting on the smallest curve radius (1 m radius), peak resultant ground reaction forces decreased to 69% (inside leg) and 83% (outside leg) of those generated on the straight path, though the outside leg difference was not statistically significant. This is direct evidence against the primary assumption that the peak resultant ground reaction forces generated during straight path sprinting are generated on flat curves.

An additional test of the constant leg force assumption was to examine whether our data relating sprint velocity and radius significantly differed from Greene's model. Our maximum velocity data provided a power curve fit with an exponent of 0.363 (95% C.I. for exponent is 0.351–0.375; Eqn 1, Fig. 7). This exponent was substantially greater than either exponent predicted by Greene for small or large radii tracks (P<0.05). In 1987, Greene revised his theory to incorporate sprinting on banked tracks. We further compared two predictions made from his later model for the velocity–radius relationship assuming no bank angle. We found that these predicted exponents again fell outside of the 95% C.I. of our fitted data (Fig. 7).

The constant leg extension force hypothesis predicts that time of foot contact would increase at smaller radii to maintain the necessary vertical impulse "*to compensate for the vectorial decrease of available vertical force*" (Greene, 1985). Time of contact generally increased in our study with smaller radii and correlated with slower sprint velocities. Our empirical data suggest, however, that the vertical ground reaction forces decreased more than would be predicted by a simple redistribution of the resultant force vector from vertical to lateral components. In other words, the decrease in peak vertical ground reaction force was not constrained by a physiological limit for maximum force production by the leg. In fact, as indicated by the smaller peak resultant forces generated during curve sprinting, each subject had ample leg extension force available to generate the necessary vertical impulses for a shorter ground contact time. We propose that the generation of ground reaction forces was constrained instead by one or more other limiting factors. To gain insight into what these limiting factors might be, we tested another simplifying assumption made by these generalized curve sprinting models, which is the symmetrical function of the legs. By investigating the function of each individual leg in greater detail, we can come closer to elucidating the mechanisms that limit performance during a complex behavior like curve sprinting and generate additional hypotheses about the nature of speed and maneuverability in legged locomotion.

Leg asymmetry

The use of the tether to externally supply the centripetal force necessary to sprint along a curved path increased maximum tangential velocity by 12% on average over the normal, untethered conditions (Fig. 3, Table 1). It also provided insight into the asymmetrical function of the legs during curve sprinting. An implicit assumption in many curve sprinting models is that both legs act symmetrically (Alexander, 1982; Howland, 1974; Keller, 1973; Mureika, 1997). We showed that the peak resultant ground reaction forces generated by the inside leg were more sensitive to track radius compared to those of the outside leg during normal curve sprinting (Eqn 1, 2). This suggests that each leg was experiencing substantially different biomechanical constraints during normal curve running with the inside leg being more severely affected. The addition of the tether eliminated these differences between legs and we observed a significant increase in sprint speed.

Just as the weakest link in a chain limits the overall performance of the chain, a force limitation in one leg can result in a reduction of maximum performance of the entire locomotor system. Given that force generation is correlated with straight path sprint speed (Weyand et al., 2000), the critical limit to curve sprinting speed is likely found in the forces generated by the inside leg. It appears that the inside leg reached some critical biomechanical threshold and limited the overall sprint speed.

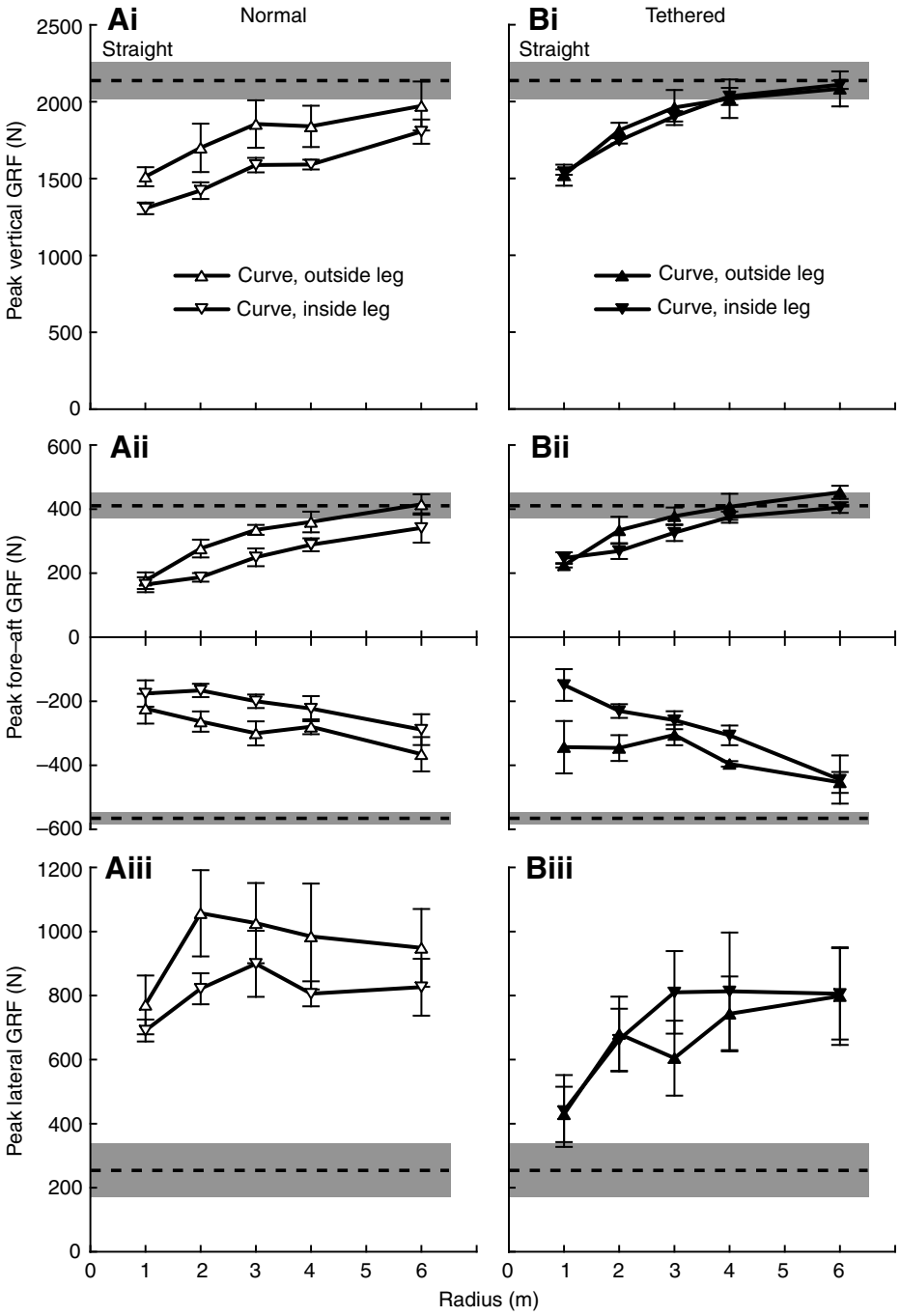

Fig. 5. Mean peak ground reaction force (GRF) components (i, vertical; ii, fore–aft; iii, lateral) for normal curve sprinting (A, open symbols) and tethered curve sprinting (B, filled symbols) as a function of curve radius. Data for each condition from the outside leg (triangles) and the inside leg (inverted triangles) are given. Fore–aft GRFs indicate both peak braking GRFs (negative) and peak propulsive GRFs (positive). Mean peak GRFs (broken lines) and s.e.m. (gray bands) during straight path sprinting are given for each case. Values are means ± s.e.m. for the same number of subjects indicated for each condition as in Table 1.

Studies of discrete 'cutting' turns may shed light on the asymmetric constraints placed on the legs during human curve sprinting. Data from running (Ohtsuki and Yanase, 1989; Ohtsuki et al., 1987; Ohtsuki et al., 1988; Rand and Ohtsuki, 2000) and walking (Hase and Stein, 1999; Orendurff et al., 2006) reveal functional differences during discrete turns made on either the outside leg or the inside leg. For discrete turns, the inside leg is less effective at making quick changes in running direction (Ohtsuki and Yanase, 1989; Ohtsuki et al., 1987; Ohtsuki et al., 1988; Rand and Ohtsuki, 2000). The inside leg also generates smaller force impulses (Ohtsuki et al., 1988) and exhibits reduced muscle activation levels (Rand and Ohtsuki, 2000) compared to the outside leg during discrete turns. Our curve sprinting study supports these previous studies. At maximal effort, a reduction in peak resultant ground reaction forces by the

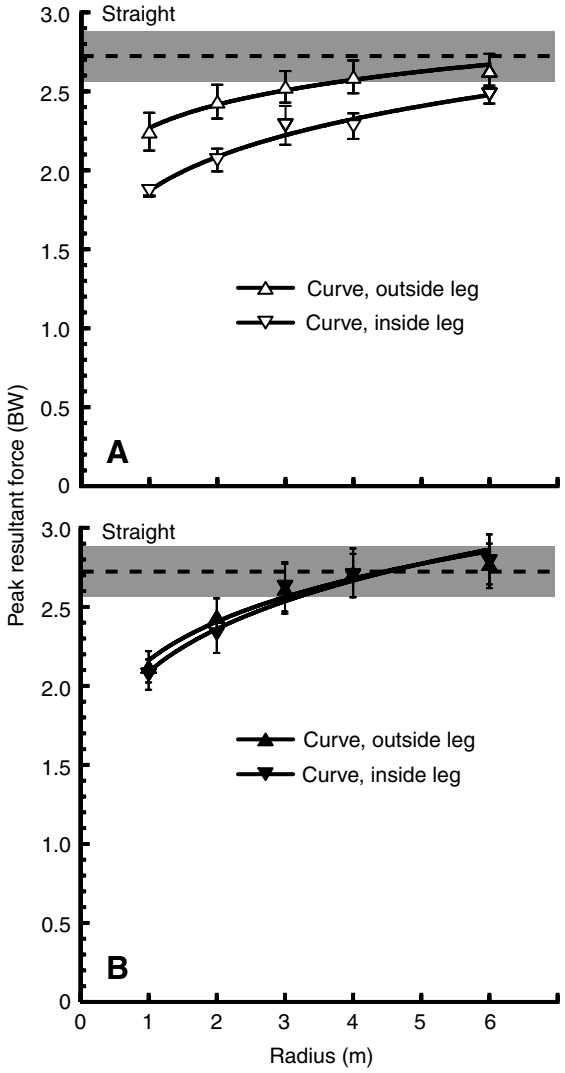

Fig. 6. Normalized peak resultant ground reaction forces (body weights, BW) for the outside leg (triangles) and inside leg (inverted triangles) as a function of radius (R) during normal curve sprinting (A) and curve sprinting with a tether (B). Contrary to current curve sprinting theory (Greene, 1985), axial leg force (represented here by resultant GRF) decreased with decreasing radius. During normal curve sprinting, the outside leg generates significantly greater axial leg force than the inside leg force (A). With the addition of an external centripetal force provided by a tether rope, however, each leg produces the same axial leg force (B). Values are means ± s.e.m. for all subjects at each radius. The broken line indicates average peak force on straight path; the gray band indicates ± s.e.m. Lines represent power fits of the outside leg (solid line) and inside leg (broken line) data. For normal curve sprinting: resultant GRF of outside leg=$2.27R^{0.091}$ (r^2=0.983); resultant GRF of inside leg=$1.87R^{0.156}$ (r^2=0.985). For tethered curve sprinting: resultant GRF of outside leg=$2.16R^{0.155}$ (r^2=0.976); resultant GRF of inside leg=$2.09R^{0.176}$ (r^2=0.977).

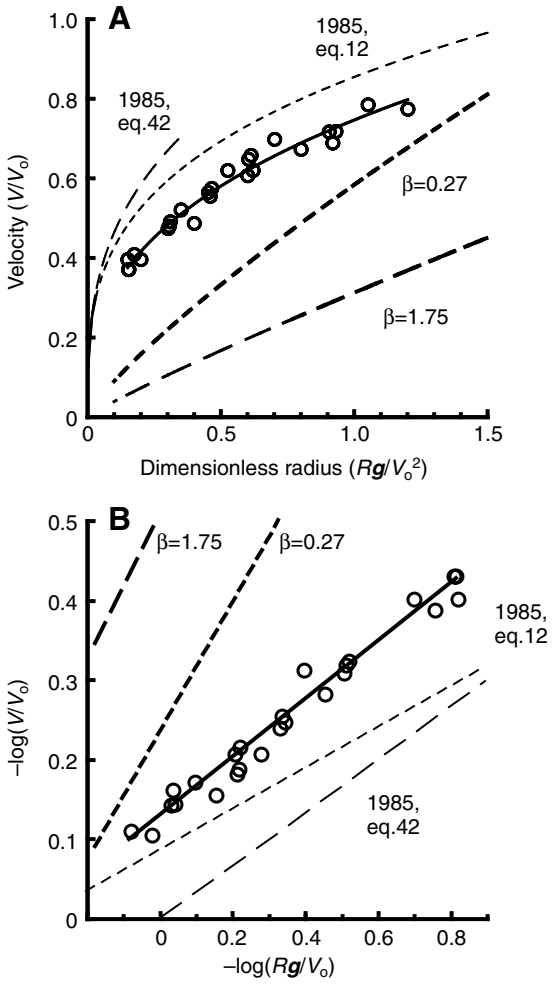

Fig. 7. Normal curve sprinting velocity data from all subjects plotted with velocities predicted by theory (Greene, 1985; Greene, 1987). Normalized velocity (V/V_o) plotted against a dimensionless radius (Rg/V_o^2) for normal curve sprinting (A) and the same data plotted after being transformed to negative log–log coordinates (B). This negative log transformation allows for ease of comparing slopes of our data against theory. Our data fit to a power curve with a significantly higher exponent than both of Greene's 1985 predictions (P<0.05) and smaller than Greene's 1987 predictions (P<0.05). Our data provide the following fit: V/V_o=0.746 $(Rg/V_o^2)^{0.363\pm0.012}$. Greene's 1985 theory for small radii [for Rg/V_o^2<0.25, thin broken line; equation 42 in Greene (Greene, 1985)] predicted a relationship of: $V/V_o=(Rg/V_o^2)^{0.333}$. Greene's theory for large radii [for Rg/V_o^2<1, thin dotted lines; equation 12 in Greene (Greene, 1985)] predicted a relationship of V/V_o=0.879 $(Rg/V_o^2)^{0.258}$. Greene's 1987 theory [for β=0.27, thick dotted lines; equation 20 in Greene (Greene, 1987)] predicted a relationship of V/V_o=0.234 $(Rg/V_o^2)^{0.812}$ or [for β=1.75, equation 20 in Greene (Greene, 1987)] predicted a relationship of V/V_o=0.505 $(Rg/V_o^2)^{0.903}$.

inside leg likely plays a significant role in limiting speed during curve sprinting.

What limits peak force generation by the inside leg?

The difficulty of understanding the limits to curve sprinting is apparent when one considers it's complex nature, where significant movements are simultaneously performed in all three anatomical planes (sagittal, frontal, transverse). Different biomechanical constraints exist in each plane of motion and can also interact with one another in a complex manner. In

Table 2. *Step length, step frequency and ground contact time for each condition*

Track	Step length (m)	Step frequency (steps s^{-1})	Ground contact time (s)
Straight	2.07±0.12	3.72±0.19	0.159±0.005
Curved radius (m)			
Outside leg			
6	1.70±0.10*	3.56±0.12	0.190±0.006
4	1.45±0.05*	3.66±0.18	0.198±0.007
3	1.41±0.07*	3.35±0.10	0.226±0.008*
2	1.18±0.08*	3.30±0.18	0.242±0.010*
1	0.80±0.04*	3.56±0.26	0.261±0.022*
Inside leg			
6	1.53±0.02*	3.88±0.13	0.203±0.008
4	1.30±0.03*	4.05±0.11	0.221±0.009*
3	1.21±0.03*	3.78±0.06	0.233±0.008*
2	1.01±0.07*	3.74±0.23	0.263±0.008*
1	0.77±0.02*	3.82±0.12	0.290±0.004*

Values are means ± s.e.m. (N=5).

*Statistically significant different to the straight path condition (P<0.05).

Symmetry was assumed on the straight path.

comparison, straight path sprinting by humans, other cursorial mammals and birds generally involves movements largely restricted to the sagittal plane, where any out of plane constraints are not likely to play an important role in determining maximum speed.

We propose that the need to optimize the alignment of the resultant ground reaction force with the long axis of the leg during sprinting is a superseding principle that guides the coupling of force constraints in all planes of motion. This has been observed in a variety of running animals under different straight path running conditions (Biewener, 1989; Chang et al., 2000; Full et al., 1991; Full and Tu, 1991; Gunther et al., 2004). Aligning the resultant force vector with the leg generally leads to a favorable minimization of joint moments, musculoskeletal stresses and associated metabolic costs (Alexander, 1991) and has been hypothesized to be a fundamental behavioral template for diverse locomotor systems (Full and Koditschek, 1999). Although we did not have sufficient 3-D kinematic data to quantify the alignment of the resultant ground reaction force with the leg, this represents a logical next step and testable hypothesis that deserves further attention. This leg alignment principle may act to couple biomechanical constraints across planes such that non-sagittal plane force constraints that were negligible during straight path sprinting are likely to significantly limit peak resultant ground reaction forces during curve sprinting.

The average vertical ground reaction force over an integral number of steps must be equal to the body weight of the sprinter. Because of this constraint, faster sprint speeds correlate with greater peak vertical ground reaction forces and less time of foot contact with the ground, as demonstrated by Weyand and colleagues (Weyand et al., 2000). We have shown here that vertical ground reaction forces were smaller at smaller radii and resulted in slower sprint speeds. But, we saw that vertical ground reaction forces decreased more than could be explained by a simple reallocation (or change in orientation) of the resultant ground reaction force vector to generate lateral, centripetal forces. Rather, the magnitude of the peak resultant ground reaction force also decreased during curve sprinting.

Muscles acting primarily to stabilize joints in the frontal plane may be inhibiting this leg extension force in the sagittal plane. Changing the angle of hip adduction has been shown to change knee extensor activity during squatting exercise (Coqueiro et al., 2005). Also, studies on submaximal discrete running turns found a discrepancy in the how non-sagittal plane joint stabilization demands increased at the knee joints, depending on which leg was used for making the turn (Besier et al., 2003; Besier et al., 2001a; Besier et al., 2001b). With no substantial change in net knee extension moments between legs in the sagittal plane, Besier and colleagues found substantial differences between the legs in frontal plane and transverse plane moments. The inside leg consistently generated greater varus moments and external rotation moments compared to the outside leg. At maximal effort, these non-sagittal plane knee joint moments may have reached critical limits, constraining the ability to increase sagittal plane extension moments. We are not aware of any similar studies of the ankle joint stabilizers. However, based on the ratios of our ground reaction force components, we would expect lean angles (as a proxy for ankle inversion angle) to be 35–40°. At these high ankle inversion angles, the inside leg ankle stabilizer muscles may have been operating near or at their critical limits as well. Stabilizing the different joints in the frontal and transverse planes during curve sprinting is a likely mechanism that limits leg extensor forces.

For example, at a given curve radius, sagittal plane leg extensor forces and frontal plane joint stabilization forces likely increase in proportion with increasing sprint speed until a physiological limit is reached in one or more muscle groups. The ratio of sagittal plane extensor muscle force to frontal plane joint stabilization muscle force is likely greatest during straight path sprinting, where speed is limited solely by the forces generated by extensor muscles. On increasingly tighter curves, this ratio probably decreases such that the absolute limit of muscle stress of the frontal plane joint stabilizers is reached at proportionately slower speeds while the extensor muscles remain well within their maximum force generating capacity. This hypothetical scenario is illustrated in Fig. 8. This could explain why we observed significantly smaller peak resultant ground reaction forces during curve sprinting compared to straight path sprinting.

Alexander suggested that at smaller radii, the coefficient of friction between the ground and the feet would limit sprint speed (Alexander, 1982; Alexander, 2002). Our subjects wore rubber-soled running shoes and sprinted on a clean asphalt track. In addition, the force platform surface was covered with a rubber matting to eliminate the risk of slipping. Although we did not measure the static coefficient of friction of our subjects' shoes on the track, typical values for rubber on asphalt range from 0.5–0.8 with running shoes in particular being on the upper end

of this scale at approximately 0.75 (Tanaka et al., 2001). We did not observe any slipping during our trials nor did any of our subjects report any fear of slipping during trials or practice sessions.

The static coefficient of friction is a ratio of shear force to normal force just before slipping occurs. 'Required coefficient of friction' or RCOF is a ratio of the shear force to normal force generated during normal locomotion without slipping and provides a relative measure of slip potential (Redfern et al., 2001). We calculated ensemble averages of RCOF across subjects at times of peak force generation (peak lateral force:peak vertical force) and found it was generally less than 0.60 in all but one condition: the outside leg at 2 m radius condition (RCOF=0.63). These ratios spanned a range of 0.45–0.63 across all radii for both legs, which were well within the range of non-slip conditions suggested in the literature.

Our subjects were likely modulating their fore–aft braking forces to control body rotation and heading direction. The necessity to control body rotation while sprinting on a curved track has received relatively little attention. Since a sprinter must perform one complete rotation of the body for each lap around the track, the angular velocity of the center of mass around the track must equal the angular velocity of the body in the transverse plane. Therefore, a sprinter's rotational velocity in the transverse plane is directly related to their sprint speed. Recently, Jindrich and colleagues suggested that braking forces generated during discrete turns in human running may serve to control rotation of the body in the transverse plane (Jindrich et al., 2006). This supports their previous findings that running insects also use this general mechanism for controlling over-rotation (Jindrich and Full, 1999). This may explain the consistent multiphasic pattern of fore–aft braking forces observed between normal and tethered curve sprinting conditions (Fig. 4). This is another example of a coupling mechanism that can add to a multi-faceted system of force generating constraints during curve sprinting.

The generation of forces on the ground by the legs during curve sprinting is a complex three-dimensional task bounded by several coupled biomechanical constraints. Maximizing the peak vertical ground reaction forces will minimize time spent on the ground and increase forward speed, as previously discussed. Lateral ground reaction forces must also be maximized to provide the centripetal force to change the momentum vector of the body and maximize forward (tangential) sprint speed, since centripetal force is proportional to the square of velocity. Fore–aft braking and propulsion forces must provide a delicate balance of maximizing forward acceleration and sprint speed while also controlling body rotation in the transverse plane. It is likely that during curve sprinting, these biomechanical constraints become inexorably coupled and cause sprinters to reach a critical limit at slower sprint speeds. To our knowledge, these speed-limiting mechanisms have not been considered in this light and warrant further study.

These multiplanar constraints are necessarily coupled for a bipedal sprinter that has only one leg to generate forces on the ground. In quadrupeds, it is possible that these constraints may become decoupled through a delegation of biomechanical tasks to different limbs. For example, trotting dogs have an asymmetric distribution of function with forelimbs performing more of the braking in the fore–aft direction while the hindlimbs perform most of the acceleration (Lee and Bertram, 1999). Six-legged runners also exhibit this specialization of tasks for each of the legs with the front legs performing most of the braking function (Full et al., 1991) while also controlling for rotation in the transverse plane (Jindrich and Full, 1999). Decoupling of the force-generating roles of the front and hind limbs during curve sprinting has been suggested as a major mechanism that allows mice (Walter, 2003) and dogs (Usherwood and Wilson, 2005) to reach greater relative curve sprint speeds compared to human curve sprinters. In this sense, bipedal sprinters such as humans and birds may be relatively slower than quadrupeds or hexapods during curve sprinting, due to an inability to decouple the additional constraints placed on them by this more complex behavior.

In summary, we have shown that maximum sprint velocity on curves is not only limited by a physiological limit to axial leg force since: (1) direct evidence indicates that maximal physiological force generation is not achieved during maximal

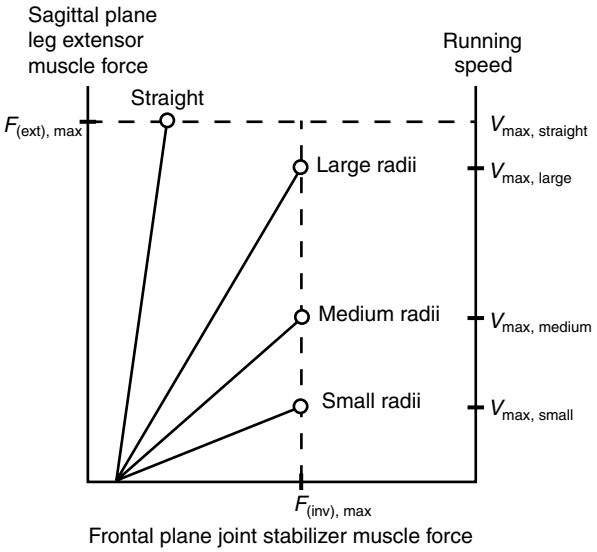

Fig. 8. Hypothesized relationship of performance constraints between a sagittal plane extensor muscle and a frontal plane stabilizer muscle (e.g. foot invertor). As track radius decreases, the ratio of extensor muscle force generation to joint stabilizer muscle force (indicated by slope of solid lines) decreases as frontal plane stabilization becomes increasingly important at these tighter curves. Along the straight path, joint stabilizers play a negligible role in limiting speed and maximum sprint speed is constrained only by a maximum extensor muscle force limit ($F_{(ext)max}$, broken horizontal line). On a curved path, however, the importance of joint stabilization in the frontal plane becomes increasingly important with smaller radii, and sprint speed may become increasingly limited by the ability of a group of joint stabilizer muscles to generate force (e.g. $F_{(inv)max}$, broken vertical line). Open circles denote the hypothetical maximum attainable sprint speed for a given track radius.

effort sprinting at all radii; (2) externally supplying centripetal forces did not increase maximum velocities on the curve to expected values and revealed the importance of the underlying asymmetry between inside and outside legs; and (3) the power fit exponent of our empirical velocity data was significantly different from Greene's theoretical predictions. Instead, we propose that several coupled biomechanical constraints placed on the stance leg during curve sprinting make the inside leg particularly ineffective at generating the forces necessary to achieve straight path sprint velocities. The ability to decouple these constraints through the redistribution of function across multiple legs in quadrupeds may explain their superior curve sprint performance compared to bipedal sprinters.

Special thanks to Kelly Campbell, who was instrumental for the data collected for this study. Thanks also to Tim Griffin, Max Donelan and Bob Full for helpful comments on the manuscript and to the UC Berkeley Statistical Consulting Services for their assistance with the statistical analyses. Thanks to Scott E. Shackleton of the UC Richmond Field Station for design and construction support of the instrumented track. The work was supported in part by a Grant-in-Aid of Research from the American Society of Biomechanics (Y.-H.C.), the UC Berkeley McNair Scholars Program (K.C.) and NIH R29-AR44688 (R.K.).

References

Alexander, R. McN. (1982). *Locomotion of Animals*. New York: Blackie Press, Chapman & Hall.

Alexander, R. McN. (1991). Energy-saving mechanisms in walking and running. *J. Exp. Biol.* **160**, 55-69.

Alexander, R. McN. (2002). Stability and manoeuverability of terrestrial vertebrates. *Integr. Comp. Biol.* **42**, 158-164.

Besier, T. F., Lloyd, D. G., Ackland, T. R. and Cochrane, J. L. (2001a). Anticipatory effects on knee joint loading during running and cutting maneuvers. *Med. Sci. Sports Exerc.* **33**, 1176-1181.

Besier, T. F., Lloyd, D. G., Cochrane, J. L. and Ackland, T. R. (2001b). External loading of the knee joint during running and cutting maneuvers. *Med. Sci. Sports Exerc.* **33**, 1168-1175.

Besier, T. F., Lloyd, D. G. and Ackland, T. R. (2003). Muscle activation strategies at the knee during running and cutting maneuvers. *Med. Sci. Sports Exerc.* **35**, 119-127.

Biewener, A. A. (1989). Scaling body support in mammals – limb posture and muscle mechanics. *Science* **245**, 45-48.

Biewener, A. A. (1990). Biomechanics of mammalian terrestrial locomotion. *Science* **250**, 1097-1103.

Chang, Y. H., Huang, H. W. C., Hamerski, C. M. and Kram, R. (2000). The independent effects of gravity and inertia on running mechanics. *J. Exp. Biol.* **203**, 229-238.

Coqueiro, K. R. R., Bevilaqua-Grossi, D., Berzin, F., Soares, A. B., Candolo, C. and Monteiro-Pedro, V. (2005). Analysis on the activation of the VMO and VLL muscles during semisquat exercises with and without hip adduction in individuals with patellofemoral pain syndrome. *J. Electromyogr. Kinesiol.* **15**, 596-603.

Full, R. J. and Koditschek, D. E. (1999). Templates and anchors: neuromechanical hypotheses of legged locomotion on land. *J. Exp. Biol.* **202**, 3325-3332.

Full, R. J. and Tu, M. S. (1991). Mechanics of a rapid running insect: two-, four- and six-legged locomotion. *J. Exp. Biol.* **156**, 215-231.

Full, R. J., Blickhan, R. and Ting, L. H. (1991). Leg design in hexapedal runners. *J. Exp. Biol.* **158**, 369-390.

Greene, P. R. (1985). Running on flat turns: experiments, theory, and applications. *J. Biomech. Eng.* **107**, 96-103.

Greene, P. R. (1987). Sprinting with banked turns. *J. Biomech.* **20**, 667-680.

Gunther, M., Keppler, V., Seyfarth, A. and Blickhan, R. (2004). Human leg design: optimal axial alignment under constraints. *J. Math. Biol.* **48**, 623-646.

Harrison, A. and Ryan, G. J. (2000). The effects of bend radius of curvature on sprinting speed and technique. In *Proceedings of the 12th Annual Congress of the European Society of Biomechanics*, pp. 358. Dublin.

Hase, K. and Stein, R. B. (1999). Turning strategies during human walking. *J. Neurophysiol.* **81**, 2914-2922.

Howland, H. C. (1974). Optimal strategies for predator avoidance: the relative importance of speed and manoeuverability. *J. Theor. Biol.* **47**, 333-350.

Jain, P. C. (1980). On a discrepancy in track race. *Res. Q. Exerc. Sport* **51**, 432-436.

Jindrich, D. L. and Full, R. J. (1999). Many-legged maneuverability: dynamics of turning in hexapods. *J. Exp. Biol.* **202**, 1603-1623.

Jindrich, D. L., Besier, T. F. and Lloyd, D. G. (2006). A hypothesis for the function of braking forces during running turns. *J. Biomech.* **39**, 1611-1620.

Keller, J. B. (1973). A theory of competitive running. *Phys. Today* **26**, 43-47.

Kram, R., Griffin, T. M., Donelan, J. M. and Chang, Y. H. (1998). Force treadmill for measuring vertical and horizontal ground reaction forces. *J. Appl. Physiol.* **85**, 764-769.

Lee, D. V. and Bertram, J. E. A. (1999). Acceleration and balance in trotting dogs. *J. Exp. Biol.* **202**, 3565-3573.

McMahon, T. A. and Greene, P. R. (1979). The influence of track compliance on running. *J. Biomech.* **12**, 893-904.

Mureika, J. R. (1997). A simple model for predicting sprint-race times accounting for energy loss on the curve. *Can. J. Phys.* **75**, 837-851.

Ohtsuki, T. and Yanase, M. (1989). Mechanical verification of the effectiveness of the first step for quick change of the forward running direction. In *Proceedings of the XII International Congress of Biomechanics* (ed. R. J. Gregor, R. F. Zernicke and W. C. Whiting), p. 237. Los Angeles.

Ohtsuki, T., Yanase, M. and Aoki, K. (1987). Quick change of the forward running direction in response to unexpected changes of situation with reference to ball games. In *Biomechanics X-B* (ed. B. Jonsson), pp. 629-635. Champaign: Human Kinetics.

Ohtsuki, T., Yanase, M. and Aoki, K. (1988). Quick change of the forward running direction and foot work in target-catching ball games. In *Biomechanics XI-B* (ed. G. De Groot, A. P. Hollander, P. A. Huijing and G. J. Van Ingen Schenau), pp. 820-825. Amsterdam: Free University Press.

Orendurff, M. S., Segal, A. D., Berge, J. S., Flick, K. C., Spanier, D. and Klute, G. K. (2006). The kinematics and kinetics of turning: limb asymmetries associated with walking a circular path. *Gait Posture* **23**, 106-111.

Rand, M. K. and Ohtsuki, T. (2000). EMG analysis of lower limb muscles in humans during quick change in running directions. *Gait Posture* **12**, 169-183.

Redfern, M. S., Cham, R., Gielo-Perczak, K., Gronqvist, R., Hirvonen, M., Lanshammar, H., Marpet, M., Pai, C. Y.-C. and Powers, C. (2001). Biomechanics of slips. *Ergonomics* **44**, 1138-1166.

Tanaka, K., Ujihashi, S., Morita, M. and Ishii, K. (2001). Correlations between the mechanical properties of running shoes and the sensory evaluations by distance runners in relation to the wear of outsole. In *Proceedings of the 5th Symposium on Footwear Biomechanics* (ed. E. Hennig and A. Stacoff), pp. 76-77. Zurich, Switzerland.

Usherwood, J. R. and Wilson, A. M. (2005). No force limit on greyhound sprint speed. *Nature* **438**, 753-754.

Usherwood, J. R. and Wilson, A. M. (2006). Accounting for elite indoor 200 m sprint results. *Biol. Lett.* **2**, 47-50.

Walter, R. M. (2003). Kinematics of 90° running turns in wild mice. *J. Exp. Biol.* **206**, 1739-1749.

Weyand, P. G., Sternlight, D. B., Bellizzi, M. J. and Wright, S. (2000). Faster top running speeds are achieved with greater ground forces not more rapid leg movements. *J. Appl. Physiol.* **89**, 1991-1999.